JOURNAL OF THEORETICAL
AND APPLIED MECHANICS
https://doi.org/10.15632/jtam-pl/201984
ONLINE FIRST

DIMENSIONAL SYNTHESIS OF SUSPENSION SYSTEM OF WHEEL-LEGGED MOBILE ROBOT[†)]

Przemysław SPERZYŃSKI*, Jacek BAŁCHANOWSKI

Wrocław University of Science and Technology, Faculty of Mechanical Engineering
Division of Fundamentals of Machine Design and Mechatronic Systems, Wrocław, Poland
*corresponding author, *przemyslaw.sperzynski@pwr.edu.pl*

This paper presents a method for selecting the common dimensions of the limb mechanism of a wheel-legged mobile robot. A synthesis task was formulated that divided it into partial stages. The solution was searched using a genetic algorithm. This accelerated the dimension selection process. The algorithm operated on integers, which made it possible to establish the accuracy of the sought basic dimensions of the limb mechanism. The objective of the synthesis was achieved, obtaining the assumed characteristics of wheel movement using the available drives. Finally, further aspects of the design of the limb mechanism of the wheel-legged mobile robot which need to be studied are presented.

Keywords: dimensional synthesis; genetic algorithm; wheel-legged robot.

1. Introduction

Wheel-legged mobile robots are hybrid systems which allow efficient movement on flat terrain and walking to overcome obstacles. The wheel suspension in the robot is a complex mechanism which needs to enable the wheel to be operated in such a way as to ensure driving (rolling and turning of the wheel – two degrees of freedom) and walking (lifting and extending of the wheel – two degrees of freedom). As a result of research work at the Wrocław University of Science and Technology, at the Faculty of Mechanical Engineering, a wheel-legged robot was developed which has four limbs enabling the above-mentioned wheel movements (Fig. 1a) (Gronowicz *et al.*, 2014).

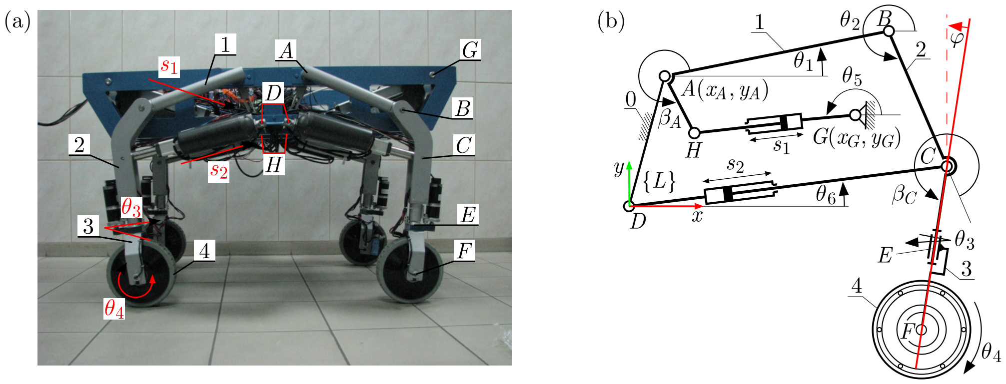

Fig. 1. (a) Prototype of the wheel-legged robot; (b) kinematic scheme of the limb.

[†)]This article was presented at the 5th Polish Congress of Mechanics and 25th International Conference on Computer Methods in Mechanics (PCM-CMM), Gliwice, Poland, September 4–7, 2023.

The aim of this paper is to present the developed method for the dimensional synthesis of a limb, which allows dimensions to be selected to ensure that the lifting motion of the wheel centre follows a trajectory close to the vertical section. The innovation of the wheel suspension used in the robot lies in the fact that, by selecting the appropriate dimensions of the system's elements, the vertical movement of the wheel can be realised using only the lifting drive, with the wheel extension drive inactive. The disadvantage of the designed limb mechanism is the tilt of the steering wheel axis away from the vertical. This tilt can cause control problems when driving. The developed geometrical synthesis method focuses on minimising the steering axis tilt angle while maintaining a rectilinear trajectory of the wheel centre.

2. Material and methods

The task of dimensional synthesis of kinematic systems is to determine the linear and angular dimensions of the elements so as to obtain the assumed law of motion of the mechanism. This is most often assumed by defining such groups of tasks as driving the elements through predefined positions, assuming relative positions of selected moving elements or realising a specific shape of the trajectory of a selected point. The geometric synthesis methods that have been developed use various algorithms or mathematical tools, and recent years have seen significant progress in the application of new methods in this area. Optimisation methods, developed on the basis of new research in artificial intelligence, are increasingly being used. A wide range of techniques for dimensional synthesis have already been explored (Kang *et al.*, 2022). These methods include, among others, fuzzy logic, neural networks (Asaeikheybari *et al.*, 2017; Malarczyk *et al.*, 2023), optimisation algorithms such as ant algorithms, simulated annealing, or genetic algorithms (GA) (Buśkiewicz, 2019; Hernández *et al.*, 2021; Shinde *et al.*, 2017; Wu *et al.*, 2020). The latter method is increasingly used due to its ease of implementation. The above-mentioned methods are replacing the classical deterministic methods concerning the optimisation problem. One reason for their use is the generally lower computational complexity (undoubtedly an advantage of the method) resulting from the fact that there is no need to calculate the derivatives of the objective function (as in the case of the Newton–Raphson algorithm).

2.1. Diagram of the robot limb

The limb of the designed wheel-legged robot has four degrees of freedom. Two of these are responsible for the movements needed to drive the robot using the wheels – that is, wheel turning and rolling. The other two movements are wheel levelling forced by actuator s_1 and walking motion forced by actuator s_2 (Fig. 1b). The main advantage of the presented limb mechanism is that the wheel movements needed to level the platform during uneven travel are performed using the levelling drive s_1, with the gait drive s_2 deactivated, fixed at a position s_2 equal to $s_{2\mathrm{lev}}$.

The stepping motion is performed by s_2 drive. By varying its length CD, the centre of the wheel F moves along an arc with centre at point B and radius BF. The wheel turning axis is located in the mechanism action plane along the section CF. This position of the axis results in the rotation of the wheel not changing the position of the wheel centre F. The choice of the geometry of the limb mechanism of the wheel-legged robot affects the inclination of the axis of the CF segment to the vertical. In the driving mode, where s_2 drive is in a fixed position, CF element is inclined in relation to the vertical axis by an angle φ (Fig. 1b). It makes maintaining a stable track difficult. The present work focusses mainly on determining the geometry of the robot suspension mechanism so that the CF segment is vertical ($\varphi = 0$) during the movement of the wheel responsible for levelling the platform.

The common dimensions of the limb mechanism are the linear and angular dimensions of the individual elements, but also s_1 and s_2 drives mounting points and their range of motion. As for the mechanism shown (Fig. 1), 12 parameters have to be selected. These are: the lengths of actuators s_1, s_2, the ranges of movement of the actuators Δs_1, Δs_2, the lengths of the elements FC, CB, AB, AH, the positions of points $A - x_A$, y_A, $D - x_D$, y_D, and the angles β_A, β_C.

2.2. Dimensional synthesis assumptions

The main objective of the synthesis is to achieve the assumed rectilinear trajectory of motion of the wheel centre – point F, forced by the movement of one drive s_1. With this movement, the drive s_2 is to be inactive, fixed at a certain length $s_2 = s_{2\text{lev}}$ (Fig. 2).

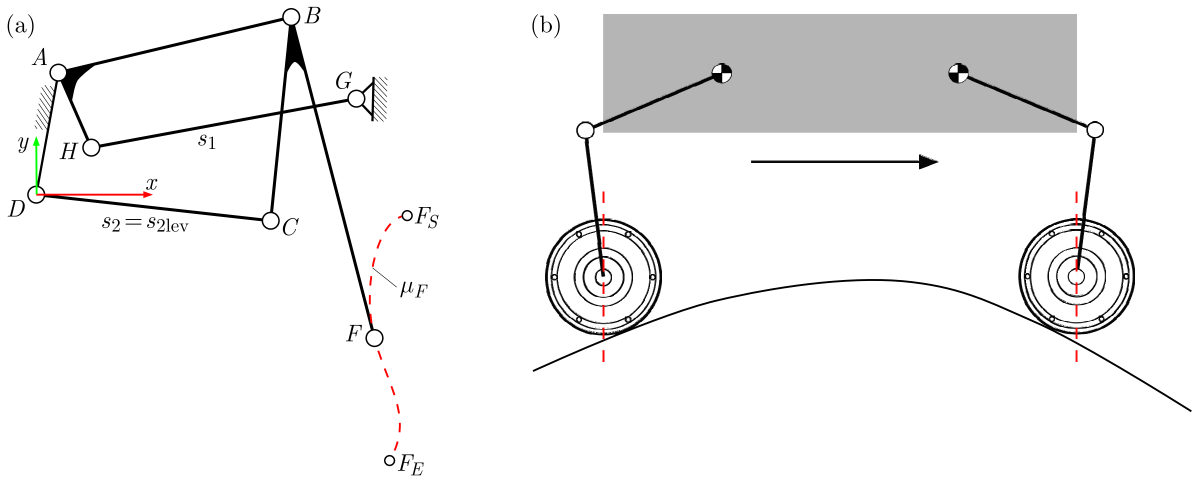

Fig. 2. (a) Wheel trajectory used to level the platform; (b) during driving on uneven terrain.

Next, to obtain the proper driving properties of the robot, it is necessary to ensure that the angle φ of orientation of the steering axis is as close to zero as possible (Fig. 3). It is undesirable for this angle to be negative (Fig. 3b).

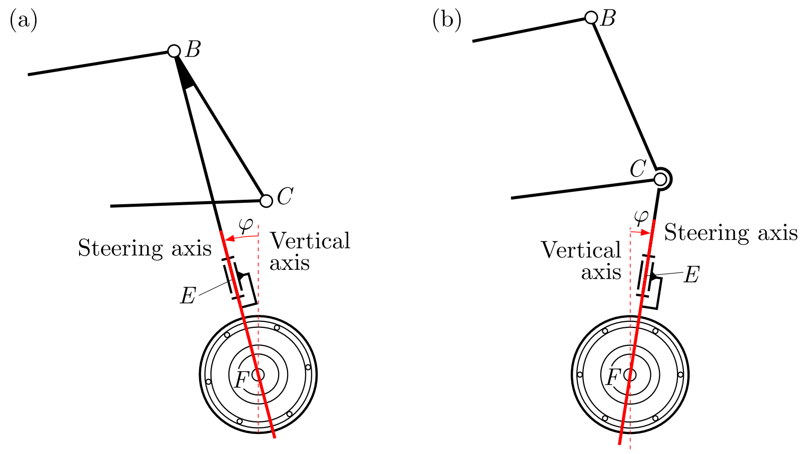

Fig. 3. Angle φ of orientation of the steering axis: (a) positive; (b) negative.

Moreover, when the gait drive s_2 is activated, the resulting limb workspace must be large enough to allow the wheel to move above the steps of a standard staircase. The most desirable case here is to obtain such a zone, which would include the profiles of two consecutive stairs (Fig. 4).

Meeting all the presented requirements is a complex task. The elaborated synthesis method consists in defining a dimension selection procedure and a set of criteria to obtain a solution that meets the requirements. The paper presents a synthesis scheme that focuses on each individual task set for the robot's suspension mechanism. At each stage of the presented synthesis method,

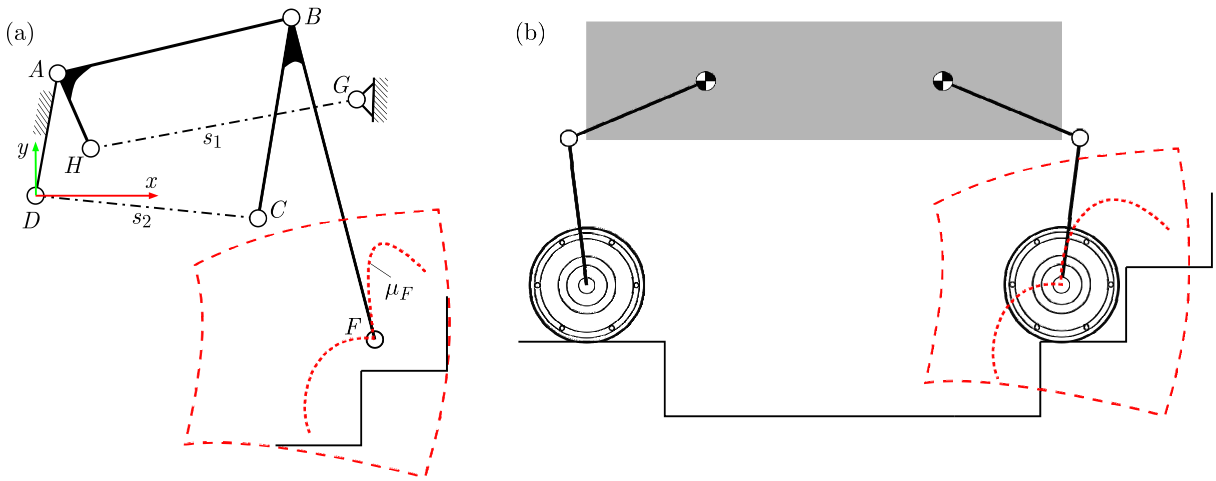

Fig. 4. (a) Robot's limb workspace, (b) while overcoming the steps.

optimization criteria focusing on single kinematic characteristics of the limb mechanism were established.

2.3. Dimensional synthesis algorithm

It was assumed that the dimensional synthesis would be divided into subtasks of basic dimension selection. The presented method allows the selection of two chosen parameters of the limb mechanism at each stage with an assumed single optimisation objective. As a result, the objective function of each stage can be visualised by plotting the area dependent on the two sought parameters.

2.3.1. Orientation angle of the steering axis orientation angle φ

The first task focuses on determining the angle φ of the steering axis orientation during wheel movement along the levelling trajectory (with the s_2 drive locked). The angle φ is given by the relation expressed by the angle of inclination of the CF segment:

$$\varphi = \theta_2 + \beta_C + 90^\circ, \tag{2.1}$$

where angle θ_2 is the orientation angle of element 2, defined as the deviation of segment BC from the horizontal (Fig. 5a).

In this stage of the synthesis, a vertical path μ_F of movement of the wheel centre F along a straight line segment from point F_S to point F_E is assumed (Fig. 5b). The parameters sought are the length CF and the x_F coordinate of the points of the vertical segment F_S–F_E. Selecting these values with the assumed μ_F motion path will determine the angles θ_6 and θ_2.

To determine the profiles of these angles, the length s_2 of the gait actuator CD is equal to the midpoint value within the range of motion $s_{2\mathrm{lev}}$. This is a predetermined value at which the limb moves in a levelling mode. The optimization task is to achieve a constant value of the orientation angle φ of the wheel axis, which is equal to zero. The objective functions were constructed based on the angle φ and defined by the following equation:

$$f_{1\mathrm{TARGET}}(CF, x_F) = \sum_i \mathrm{rms}\,(\varphi_i)\,, \tag{2.2}$$

where the function rms determines the root mean square error of the discretely defined φ angle profile. The assumed trajectory μ_F is divided into **n** points F_i $(x_{F_i},\, y_{F_i})$ for $i = 1, ..., n$ (where

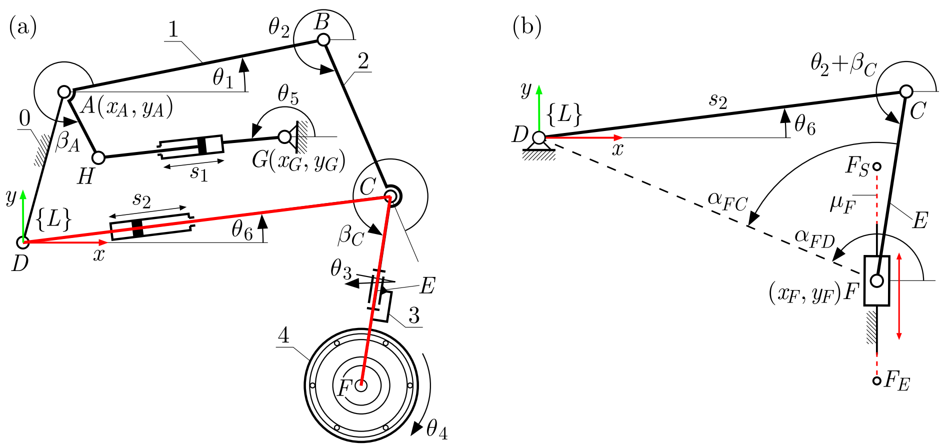

Fig. 5. (a) Selection of parameters defining the steering axis angle;
(b) kinematics parameters defining φ angle.

$F_1 = F_S$ and $F_n = F_E$) and the inclination angles θ_6 and θ_2 of the two-link CD and CF mechanism are determined at each of the assumed points F_i. The orientation $\theta_2 + \beta_C$, defining the inclination angle φ of the CF link, is calculated based on the following equation:

$$\theta_2 + \beta_C = \alpha_{FD} - \alpha_{FC} + \pi, \tag{2.3}$$

where α_{FD} represents the inclination of the FD segment at the given point F_i, and α_{FC} is the internal angle of the FDC triangle (Fig. 5b). The orientation of the FD segment, with the wheel centre F fixed at a specific position, is defined by:

$$\alpha_{FD} = \arctan \frac{y_D - y_{F_i}}{x_D - x_{F_i}}, \tag{2.4}$$

the inner angle α_{FC} of the FDC triangle was determined from the analogous relationship:

$$\alpha_{FC} = \arctan \frac{\sin \alpha_{FC}}{\cos \alpha_{FC}}, \tag{2.5}$$

where the cosine of the angle α_{FC} of the FDC triangle is determined from the cosine theorem:

$$\cos(\alpha_{FC}) = \frac{\Delta}{2 \cdot CF \cdot DF}, \tag{2.6}$$

where $\Delta = CF^2 + DF^2 - CD^2$ and the sine of the angle α_{FC} is calculated based on the trigonometric identity:

$$\sin(\alpha_{FC}) = \frac{\sqrt{(2 \cdot CF \cdot DF)^2 - \Delta^2}}{2 \cdot CF \cdot DF}. \tag{2.7}$$

In this way, for the assumed n positions of point F, the characteristics of α_{FD} from Eq. (2.4) and α_{FC} from Eq. (2.5) are obtained. By substituting them into Eq. (2.3) and then into Eq. (2.1), n values of the angle φ are determined. The calculated angles α_{FD} and α_{FC} define the positions of point C_i corresponding to the assumed positions of the wheel centre F_i:

$$(x_{C_i}, y_{C_i})^{\mathrm{T}} = (x_{F_i}, y_{F_i})^{\mathrm{T}} + CF \cdot (\cos(\alpha_{F_iD} - \alpha_{F_iC}), \sin(\alpha_{F_iD} - \alpha_{F_iC}))^{\mathrm{T}}, \tag{2.8}$$

which is essential for the subsequent synthesis step.

To search for the parameters CF and x_F that define the criterion $f_{1\mathrm{TARGET}}$ (Eq. (2.2)), a genetic algorithm was employed. The input data for the algorithm include the number of sought parameters, their value ranges, and the optimisation goal function. This concise set of information allows the search for solutions to commence. Initially, the algorithm randomly generates solution sets, which are then evaluated based on the specified criterion. Subsequently, in the algorithm main loop, the drawn sets are subjected to certain modifications. The algorithm usually terminates after a specified number of steps or when the discovered solutions do not differ significantly between iterations. To set the resolution of the achieved dimensions, the defined parameter ranges were discretised with a specified distribution. The algorithm operates with integer variables that define the dimension values within the chosen range.

2.3.2. Trace of point B in the BC suspension arm

The next synthesis step involves selecting the geometry of element 2. The sought parameters are the BC segment and the angle β_C (Fig. 6a). The motion of the mechanism is driven by the movement of the wheel centre F along the prescribed trajectory μ_F. When determining the length of the BC segment and the angle β_C, the trajectory of point B is obtained (Fig. 6b), which undergoes further evaluation in subsequent synthesis steps.

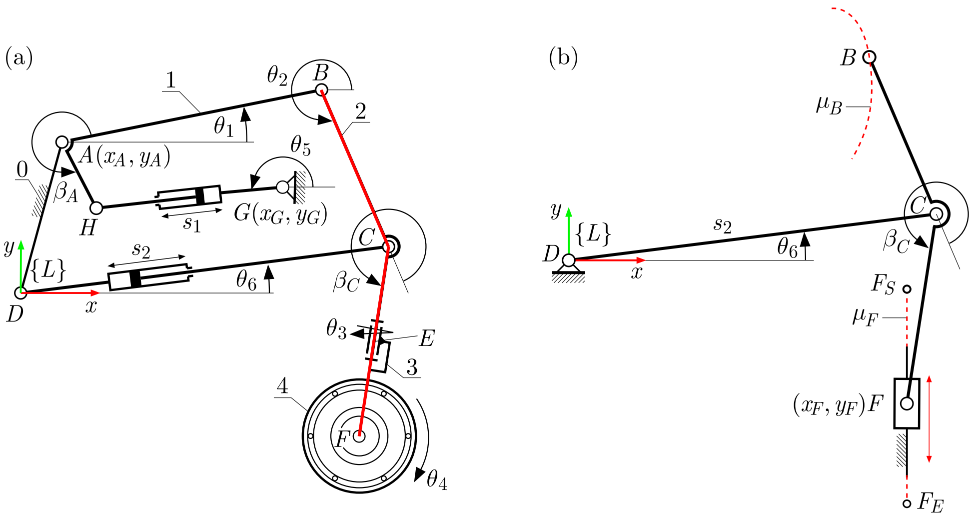

Fig. 6. (a) Selection of coupler parameters; (b) BC length and angle β_C, which determines the trajectory of point B.

The position of point B is given by the following relation:

$$(x_{B_i}, y_{B_i})^{\mathrm{T}} = (x_{C_i}, y_{C_i})^{\mathrm{T}} - BC \cdot (\cos(\theta_2), \sin(\theta_2))^{\mathrm{T}}, \tag{2.9}$$

where the angle θ_2 is determined from relation (2.3), and the position of point C is determined based on Eq. (2.8).

Point B is the point of the upper suspension arm, which has a fixed rotation centre at point A. The search criteria for the parameters BC and β_C were defined to ensure that the trajectory of point B, denoted as μ_B, closely approximates an arc. Determining the parameters of the arc (radius and centre) that approximate the μ_B trace will provide a solution to the search for point A of the suspension arm mount and its AB length. Finding the relationship that defines the curvature of the path μ_B passing through the specified points B_i was the next step in the synthesis.

2.3.3. Curvature of the point B trajectory

In the next step of the synthesis, the curvature of the trajectory of point B was determined. In the previous step, a set of B_i points corresponding to the assumed positions of the centre of the wheel centre F_i was obtained. A spline defined from a group of third-degree polynomials was drawn for each segment $\langle B_i, B_{i+1}\rangle$ through the B_i points (Fig. 7).

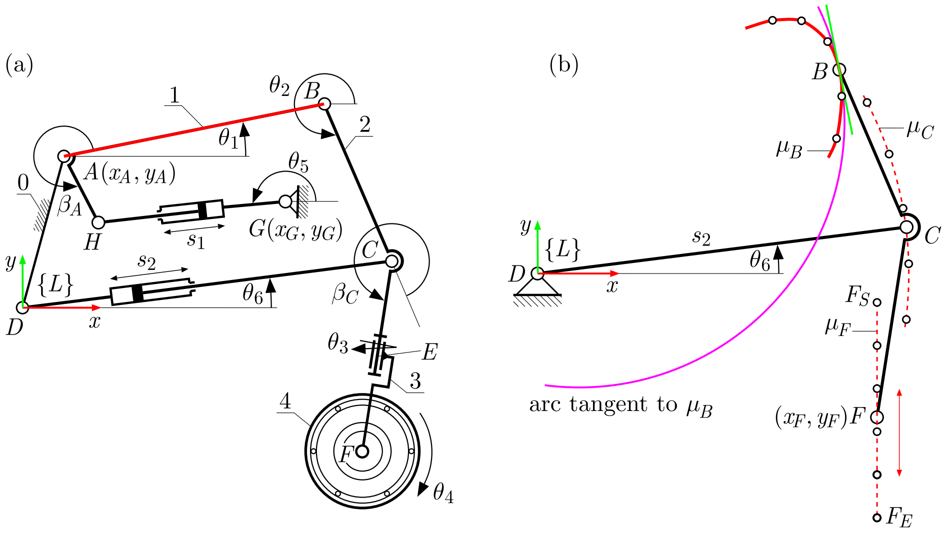

Fig. 7. (a) Upper arm parameters; (b) based on the curvature of the trace of point B.

The equation of the curve μ_B depending on the parameter u, taking values in the interval $u \in \langle 0, 1\rangle$, passing through the given points B_i was divided into segments. Each point B_i was assigned a value of the parameter u equal to u_i. The equation of the curve between two consecutive points B_i and B_{i+1} is expressed as follows:

$$\begin{aligned} x_{B_i}(u) &= p_{x3i}(u-u_i)^3 + p_{x2i}(u-u_i)^2 + p_{x1i}(u-u_i) + p_{x0i} \\ y_{B_i}(u) &= p_{y3i}(u-u_i)^3 + p_{y2i}(u-u_i)^2 + p_{y1i}(u-u_i) + p_{y0i} \end{aligned} \qquad \text{for} \quad u \in \langle u_i, u_{i+1}\rangle, \tag{2.10}$$

where the parameters u_i were determined by dividing the interval of the u values into n-equal intervals ($u_i = i/n$), and the coefficients p_{xji}, p_{yji} defined a polynomial for the parameter u from the interval $\langle u_i, u_{i+1}\rangle$. For the pair of points B_i and B_{i+1}, separate polynomial equations defined by the coefficients p_{xji} and p_{yji} were determined. For a parameter u equal to u_i, the determined parametric curve is to pass through the defined point B_i. This determines the parameters p_{x0i} and p_{y0i}, which are equal to the coordinates of the B_i points:

$$p_{x0i} = x_{B_i}, \qquad p_{y0i} = y_{B_i}. \tag{2.11}$$

The successive p_{xji} coefficients were determined so that the functions $x_{B_i}(u)$ were of class C2. The need to obtain the continuity of the first- and second-order derivatives of the parametric functions with respect to the parameter u made it possible to determine the succeeding equations:

$$\begin{aligned} &x_{B_i}(u = u_{i+1}) = x_{B_{i+1}}(u = u_{i+1}), \\ &\frac{\mathrm{d}x_{B_i}}{\mathrm{d}u}(u = u_{i+1}) = \frac{\mathrm{d}x_{B_{i+1}}}{\mathrm{d}u}(u = u_{i+1}), \qquad \frac{\mathrm{d}^2x_{B_i}}{\mathrm{d}u^2}(u = u_{i+1}) = \frac{\mathrm{d}^2x_{B_{i+1}}}{\mathrm{d}u^2}(u = u_{i+1}). \end{aligned} \tag{2.12}$$

Parameters p_{yji} were determined from analogous boundary conditions for the functions $y_{B_i}(u)$. The derivative of the polynomial equations of the parametric equation $x_{B_i}(u)$ is defined by the following equation:

$$\begin{aligned} \frac{\mathrm{d}x_{B_i}}{\mathrm{d}u} &= 3 \cdot p_{x3i}(u-u_i)^2 + 2 \cdot p_{x2i}(u-u_i) + p_{x1i}, \\ \frac{\mathrm{d}^2x_{B_i}}{\mathrm{d}u^2} &= 6 \cdot p_{x3i}(u-u_i) + 2 \cdot p_{x2i}. \end{aligned} \tag{2.13}$$

The tangent vector $\mathbf{t}_i$ to the parametric trajectory μ_B at point B_i was obtained from the first derivative of the polynomial equation:

$$\mathbf{t}_i = (p_{x1i}, p_{y1i})^{\mathrm{T}}. \tag{2.14}$$

The normal vector $\mathbf{n}_i$ rotated to the tangent by $\pi/2$ was determined from the second derivative:

$$\mathbf{n}_i = (2p_{x2i}, 2p_{y2i})^{\mathrm{T}}. \tag{2.15}$$

The tangent and normal vectors to the resulting approximated trajectory of point B allowed the curvature κ of the trace μ_B to be determined at the given points B_i:

$$\kappa = 2\frac{p_{x1i}p_{y2i} - p_{y1i}p_{x2i}}{(p_{x1i}^2 + p_{y1i}^2)^{3/2}}. \tag{2.16}$$

2.3.4. Centre of point B trajectory curvature

The consequence of determining the curvature of the trace of point B is to write a circle tangent to the trace at the given point B_i. The radius of the circle r, tangent to the trace of point B, is equal to the inverse of the curvature κ, $r = 1/\kappa$. By determining the circles tangent to the trajectory μ_B for each point B_i, the set of points A_i forming the trace μ_A of the centre of curvature of the trace of point B was attained (Fig. 8).

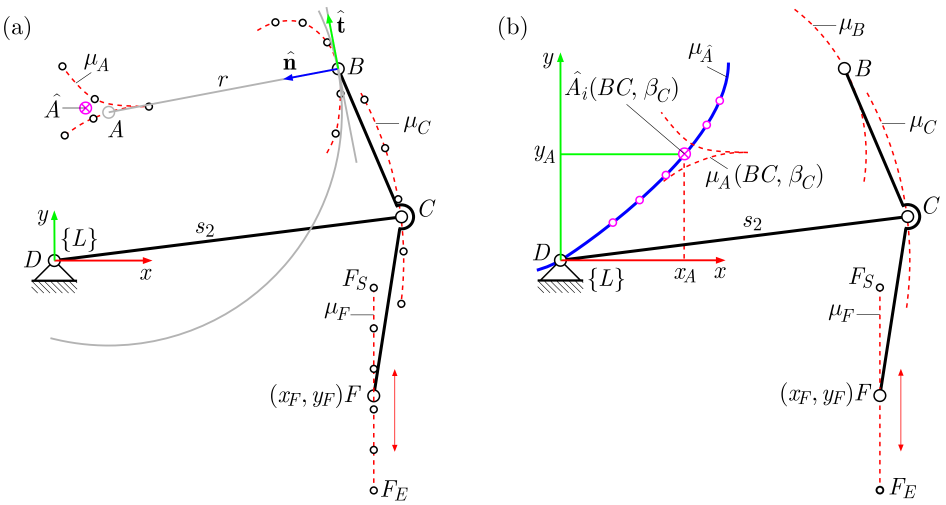

Fig. 8. (a) Point A trajectory, which is the centre of the B trace curvature κ; (b) $\mu_{\widehat{A}}$ trace of points $\widehat{A}$ corresponding to various values of BC and β_C parameters.

The trajectory μ_A of the determined centre of curvature of the trajectory μ_B composed of the points A_i is evaluated. The closer the determined trace μ_B approaches the curve, the more the points A_i will be concentrated around a single point $\widehat{A}$ $(\widehat{x}_A, \widehat{y}_A)$. The objective function was determined as follows:

$$f_{2\mathrm{TARGET}}(BC, \beta_C) = \sum_i \sqrt{(x_{A_i} - \widehat{x}_A)^2 + (y_{A_i} - \widehat{y}_A)^2}, \tag{2.17}$$

where $(\widehat{x}_A, \widehat{y}_A)$ is a point with mean coordinates from the positions of the points A_i – the centre of curvature of the trace μ_B.

A genetic algorithm was run looking for the dimensions of element 2, length BC and angle β_C, given the objective function $f_{2\mathrm{TARGET}}$ (2.17) for a fixed length $BC \neq 0$. The search was for a value of angle β_C such that the trajectory μ_A of the centre of curvature of the trace μ_B is centred around a single point. There are two points fixed to the element 2: C and F, whose trajectory has a constant trace curvature κ. Curvature of point C equals to $\kappa = 1/CD$, while F has zero curvature of the trace since it moves along a straight-line segment μ_F. The solution is sought where point B will be distant from point C and the centre of the curvature of the trace μ_B of point B will be located above point D. Performing the search for values in the range of the parameter BC resulted in obtaining a set of solutions of the position of the point $\widehat{A}(BC)$ depending on the assumed values of BC. This set was arranged in a specific curve $\mu_{\widehat{A}}$ marked in blue (Fig. 8).

On the basis of the obtained $\mu_{\widehat{A}}$ curve, the attachment point A of member 1 was determined. The design conditions defined the maximum allowed distance between point A and point D along the Y-axis. Taking the height of point A – parameter y_A, the x_A position of point A was read off from the obtained $\mu_{\widehat{A}}$ curve.

2.3.5. Levelling drive parameters s_1

In the next stage of the synthesis, the range of rotation of the rocker arm AB was determined from the orientation of section AB_1 (the highest point B_i corresponding to the given point F_S) and the orientation of section AB_n (the lowest point B_i corresponding to the given point F_E). It was assumed that, in the midpoint position AB_{mid} between AB_1 and AB_n, the levelling drive s_1 will take the value $s_{1\text{mid}}$ and be positioned at a right angle to the crank AH. Mounting point G will therefore be placed on the line μ_{G1}, perpendicular to AB_{mid} (Fig. 9).

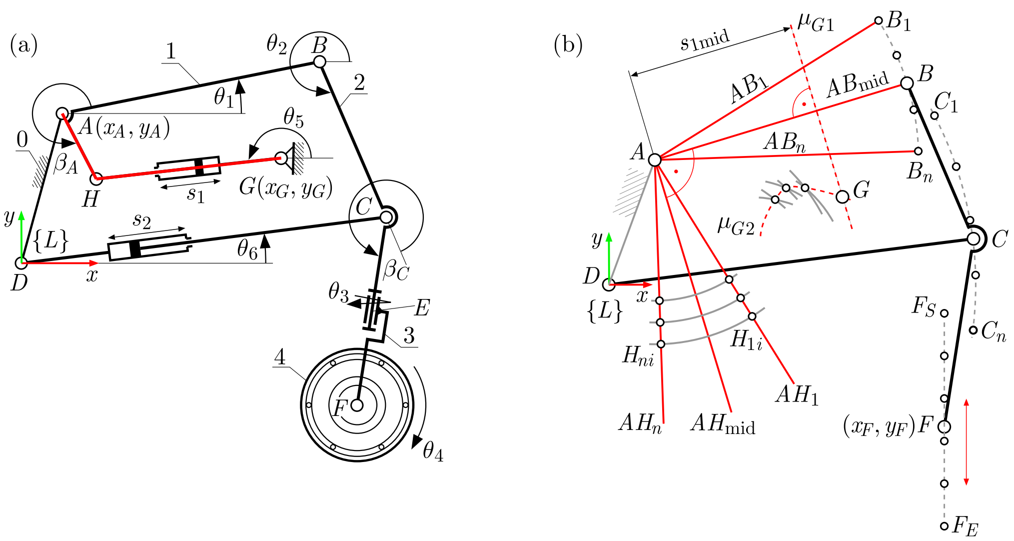

Fig. 9. (a) Lever AH and levelling drive parameters; (b) curves μ_G determining position of point G.

The initial positions H_{1i} and the final positions H_{ni} of point H were determined for a fixed length AH_i and the range of angular movement of element 1 taken from points B_1 and B_n. The position of point G_i (corresponding to the fixed value of AH_i) was determined at the intersection of circles of minimum and maximum actuator extension radius s_1 drawn from points H_{1i} and H_n. Taking successive values of AH_i from the adopted AH length range, the trace μ_{G2} of point G was obtained from the G_i points. The intersection of this trace with the previously determined straight line μ_{G1} gives the solution to determine the mounting point G of the levelling drive s_1.

2.3.6. Limb mechanism workspace

The developed method of dimensional synthesis allows one to obtain the geometry of the robot limb mechanism. The boundary of the working zone defined by the set of all positions of the centre of the wheel F was determined by fixing the positions of this point at given positions of the levelling drives s_1 and the walking drive s_2. The beginning of the curve is at point F corresponding to the configuration of the mechanism defined by the minimum positions of the levelling drive $s_1 = s_{\min}$ and the walking drive $s_2 = s_{\min}$. The s_2 drive values were successively increased up to the maximum extension value $s_2 = s_{\max}$. The levelling drive s_2 was then tilted to the value $s_2 = s_{\max}$. This resulted in obtaining the upper and right limits of the workspace. The lower limit was obtained by fixing the position of the F point by changing the stepping drive s_2 to the minimum value $s_2 = s_{\min}$. In the last step, by reversing the levelling drive s_1 to the boundary curve of the minimum value $s_1 = s_{\min}$, the workspace boundary curve was closed (Fig. 10).

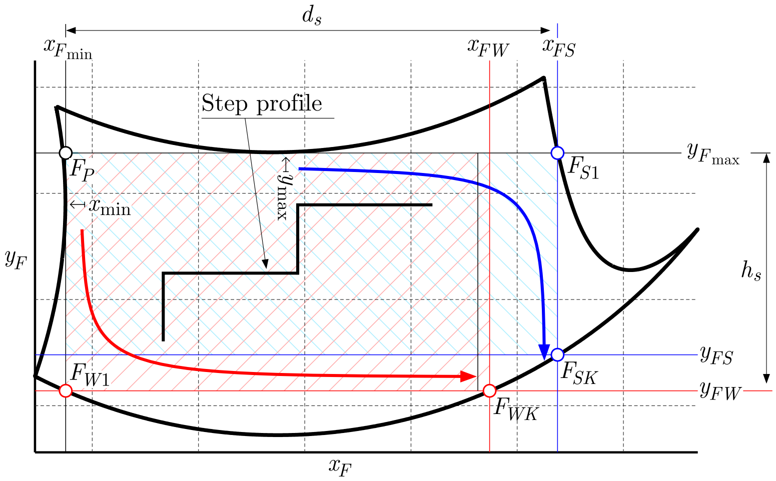

Fig. 10. Analysis of the workspace of the mechanism.

The assumptions made in the introduction determine that the resulting zone should encompass a rectangle twice the height and width of a standard staircase (Fig. 10). A horizontal tangent to the upper boundary of the workspace of the limb was defined and a vertical tangent to the left boundary of the workspace were defined. The intersection of these tangents gives the initial vertex of the rectangle inscribed in the workspace of the robotic limb. The intersection of the horizontal tangent with the right boundary gives the point F_{S1}, and the vertical line drawn from it gives the vertex F_{SK}. Whereas the intersection of the vertical tangent with the lower boundary of the workspace gives the point F_{W1}, and the horizontal line guided from it gives the vertex F_{WK}. The rectangle defined on the vertices (F_P, F_{SK}) has the maximum width d_s from the F_P point. On the other hand, a rectangle defined on the vertices (F_P, F_{WK}) is characterised by the maximum height h_s.

In such rectangles of height h_s and length d_s within the boundaries of the workspace, the profile of the staircase can be entered by checking the dimensions of the zone.

3. Results

The developed method of dimensional synthesis enabled obtaining a new limb mechanism of a wheel-walking robot. Starting from certain assumptions by performing the successive steps of the presented synthesis method, the basic dimensions of the mechanism were achieved.

In the dimensions of the first step, the CF and the position of the F-point trajectory x_F were determined for the assumed length of the walking actuator s_2 and the height of the centre of the rectilinear trajectory of the wheel centre (y_{FS}, y_{FE}). The length of the s_2 actuator was set at the value of the centre of the $s_{2\text{mid}}$ actuator, $CD = 0.425\,\text{m}$. Next, the range of motion of the wheel level was set to $0.3\,\text{m}$, from the initial value of $y_{FS} = -0.025\,\text{m}$ to the final value of

$y_{FE} = -0.325$ m. The parameters sought were the length of CF in the range (0.2 m; 0.5 m) and the position of the set trajectory x_F in the range (0.35 m; 0.55 m). The set trajectory was divided into 10 points F_i. The plane of the objective function as a function of the search parameters CF and x_F was plotted, and the course of the angle φ of the orientation of the CF member uniformly distributed around the search value zero was obtained (Fig. 11).

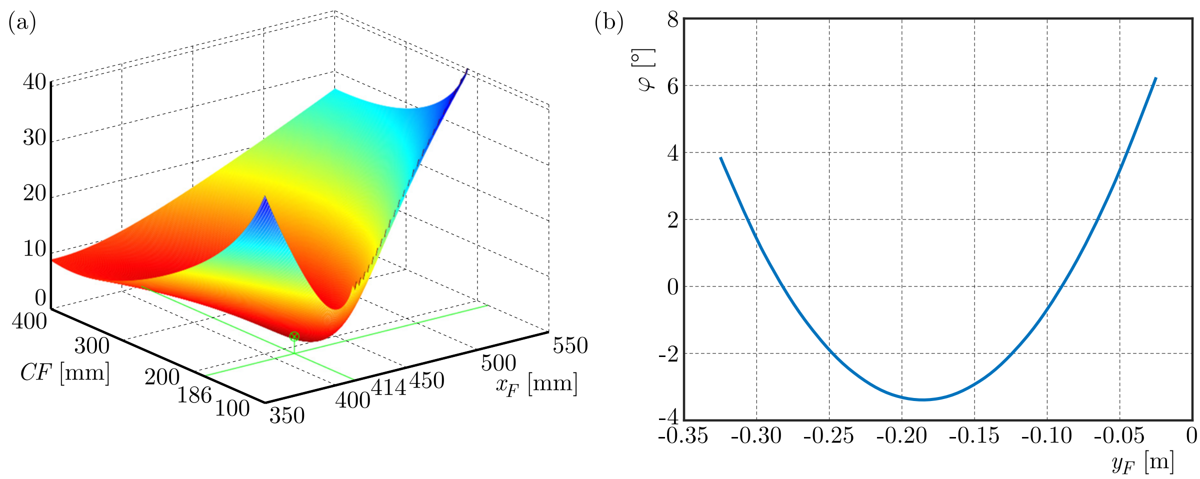

Fig. 11. (a) $f_{1\mathrm{TARGET}}$ target function dependent on CF parameters and x_F position; (b) obtained φ angle.

The trace $\mu_{\widehat{A}}$ of the point $\widehat{A}$ was then determined. The range of BC length values (from 0.001 m to 0.3 m) was assumed, and the corresponding value of β_C in the range (90°, 270°) was searched for, for which the μ_A trace of the centre of curvature of the μ_B trace was centered at a single point $\widehat{A}$. The search was carried out using the genetic algorithm and the objective function $f_{2\mathrm{TARGET}}$ (2.17). Taking BC values from a fixed range, the trajectory of the point $\widehat{A}$ (curve $\mu_{\widehat{A}}$ in blue – Fig. 12a) was determined. The maximum height between points A and D was set to 0.1 m. The coordinates of the control arm mount are equal to the intercept of the horizontal straight line $y_A = 0.1$ m and the $\mu_{\widehat{A}}$ curve (Fig. 12a).

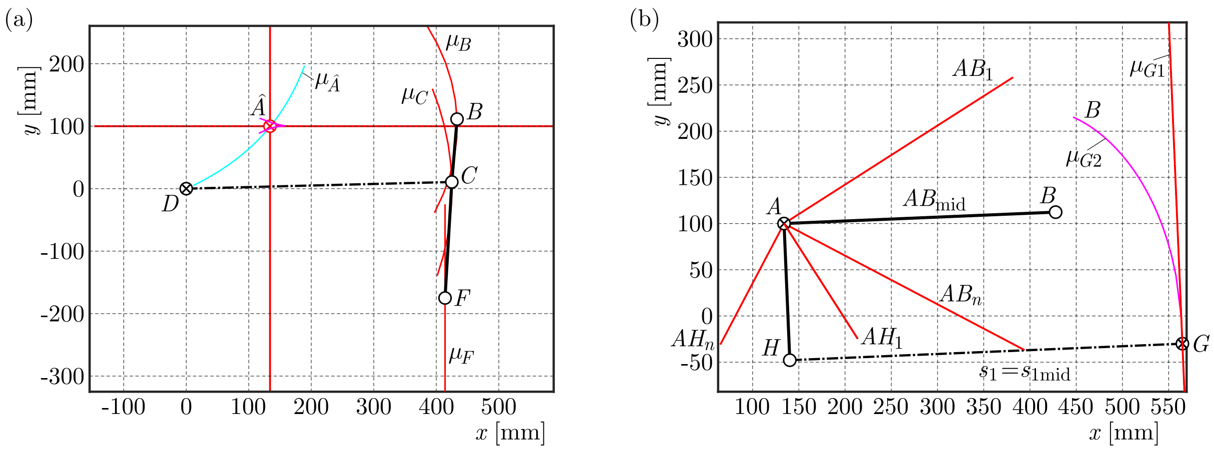

Fig. 12. (a) Trajectory $\mu_{\widehat{A}}$ of AB suspension arm 1 mount; (b) levelling drive s_1 mount point parameters.

In the next step of the synthesis, the parameters of the AH arm and the mounting of the levelling drive s_1 were determined according to the established method (Fig. 12b). The middle length of the levelling actuator $s_{1\mathrm{mid}}$ was assumed to be equal to 0.425 m. The line μ_{G1}

was drawn perpendicular to the section AB in the AB_{mid} orientation at a distance $s_{1\mathrm{mid}}$ from point A. Subsequently, for the determined lever lengths $AH_i \in \langle 0.1; 0.3\rangle$ m, the initial positions H_{1i} and final H_{ni} of the H point were obtained, corresponding to the orientation of element 1 in the AB_1 and AB_n positions. At the intersection of the circle with center H_{1i} and radius $s_{1\,\min}$ and the circle with center H_{ni} and radius $s_{1\,\max}$, points G_i corresponding to the assumed length AH_i were gained. The trace μ_{G2} was carried out through the G_i points. The intersection of this trace μ_{G2} with the line μ_{G1} set the location of point G at $(-0.03\,\mathrm{m}; 0.565\,\mathrm{m})$.

The trajectory of the centre of the μ_F wheel was obtained for the dimensions of the mechanism chosen in this way. The rotation of element 1 from orientation AB_1 to AB_n was assumed with a fixed stepping drive s_2 of 0.425 m (Fig. 13a). The size of the workspace of the mechanism was analysed with the proposed rectangle inscription method. The result was a rectangle with height h_s equal to 0.231 m and width d_s equal to 0.402 m (Fig. 13). This makes it possible to estimate the size of the obstacle the robot will be able to overcome.

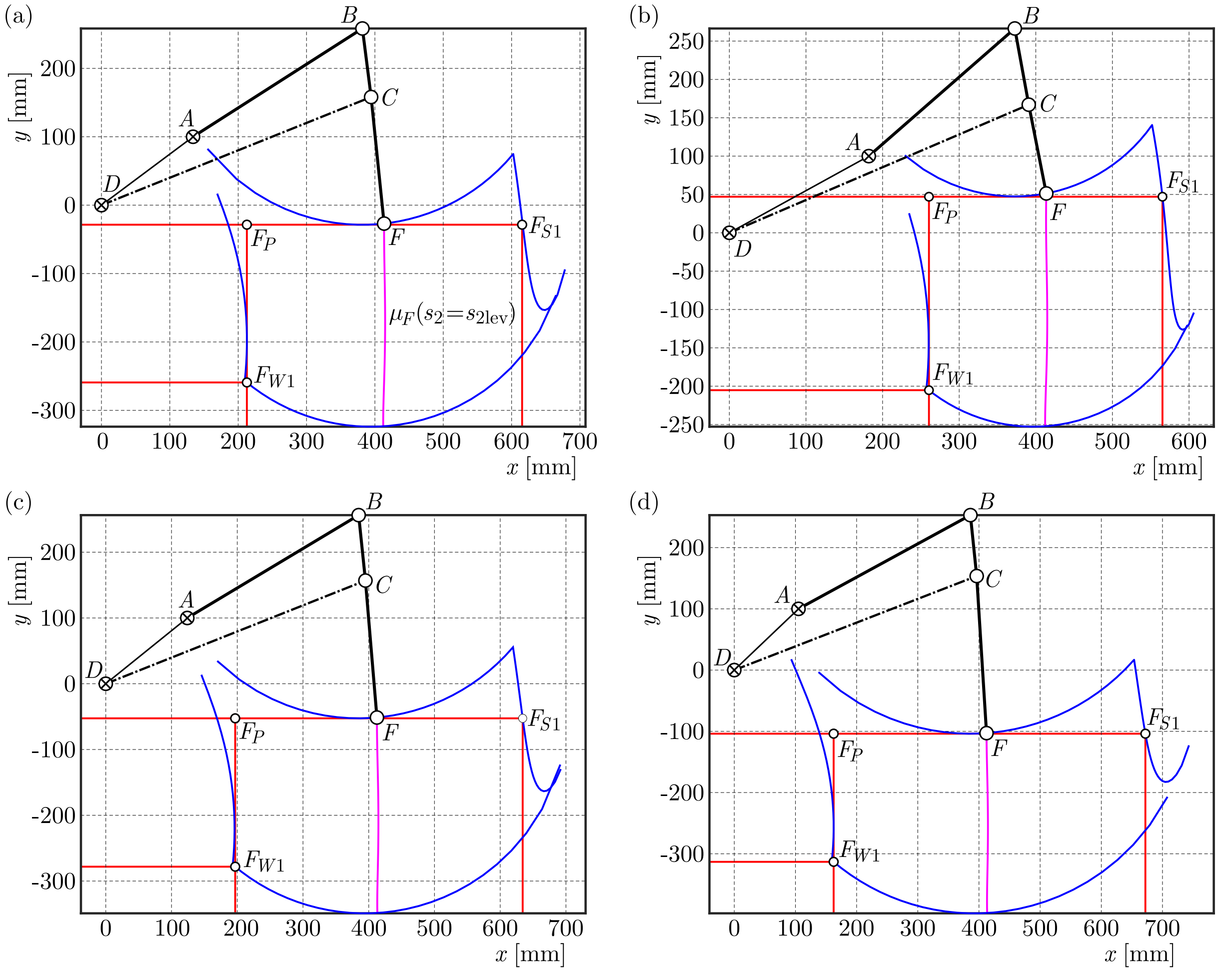

Fig. 13. Solutions obtained by the presented synthesis method for different assumed levels of the FS and FE wheel.

The synthesis of the limb mechanism was performed for different initial values of the trajectory level y_{FE} and y_{SE} and is shown in Fig. 13. The synthesis steps described were performed for the specified actuator length $s_{2\mathrm{lev}} = 0.425$ m and for four ranges of the height of the wheel centre motion trajectory μ_F. In addition to the presented case $(y_{F1} \in \langle -0.325; -0.025\rangle\,\mathrm{m})$, three additional ranges of wheel centre motion were assumed in the following intervals: $y_{F2} \in \langle -0.25; 0.05\rangle$ m, $y_{F3} \in \langle -0.35; -0.05\rangle$ m, and $y_{F4} \in \langle -0.4; -0.1\rangle$ m (Figs. 13b–d).

The basic dimensions obtained for the limb mechanism are collected in Table 1.

Table 1. Basic dimensions of the limb mechanism obtained by the proposed synthesis method.

No.	x_F [m]	CF [m]	BC [m]	β_C [°]	AB [m]	x_A [m]	AH [m]	y_G [m]	x_G [m]	h_s [m]	d_s [m]
1	0.416	0.186	0.101	−1.4	0.294	0.134	0.148	−0.03	0.565	0.231	0.402
2	0.414	0.118	0.101	0.8	0.253	0.182	0.125	0.009	0.615	0.251	0.305
3	0.414	0.209	0.1	−1.1	0.304	0.124	0.153	−0.04	0.553	0.224	0.438
4	0.414	0.257	0.1	−2.3	0.32	0.105	0.162	−0.052	0.533	0.209	0.508

4. Conclusions

This paper presents the fundamentals of the method of dimensional synthesis of the wheel-legged robot limb. The presented method for selecting basic dimensions of the mechanism requires determining the motion of the wheel (μ_F trace) and the orientation angle φ of the turning axis. The synthesis procedure is divided into stages in which at most two parameters are searched for. This allows visualisation of the adopted objective functions. The method uses a genetic algorithm operating on integer variables. This makes it possible to significantly speed up the search. In addition, it is possible to determine the accuracy of the searched parameter values. This is extremely helpful in the later stage of the assembly of the limb mechanism, where one has a strictly defined manufacturing technology.

The synthesis method resulted in the geometry of the limb mechanism of the wheel-legged robot that meets the adopted assumptions. The expected characteristics of the steering axis angle φ were obtained, the trace of which is close to the assumed constant value equal to zero. The trajectory of the centre of the wheel when the stepping drive is locked in the $s_2 = s_{2\text{lev}}$ position is quasi-rectilinear. The determined boundaries of the working zone cover the area into which it is possible to write the profile of a standard-sized staircase. Adopting the principle that the target functions depend on at most two parameters in each step of the synthesis allows their visualization and helps interpret the results. At the stage of searching for the wishbone attachment – point A, a trajectory of the point $\widehat{A}$ clustering a set of points A_i for different determined lengths of the BC segment was obtained. The approximate trajectory $\mu_{\widehat{A}}$ is a third-order polynomial curve. To determine the parameters of this polynomial, a minimum of five positions of points $\widehat{A}_i$ must be derived, which speeds up the dimension selection process.

The adopted method of dimensional synthesis of the limb has been divided in a way that allows it to be modified within one step of dimension selection, without affecting the other steps. The paper presents the case of searching for a rectilinear trajectory needed in the task of levelling a robot platform. It is possible to perform a synthesis for other assumed trajectories of wheel centre motion. The described method is based on the description of the μ_B trajectory using splines. If the spline description is changed, the curvature κ of the μ_B trace and the trace of the centre of curvature μ_A will change as a result. In the next stage of the dimension selection study, it is worth investigating the method of approximating an arc based on a set of B_i points. In this case, the determined arc parameters directly define the length AB and the position of point A without determining the curvature κ.

The presented method of dimensional synthesis provided an acceptable solution to the task of selecting the basic dimensions of the mechanism. Dividing the method into steps allows changes to the method within a given synthesis step. The developed synthesis method can be easily modified by changing the optimisation objective function or the algorithm used to find the optimal solution of the dimensions of limb mechanisms having different structures.

References

1. Asaeikheybari, G., Lafmejani, A.S., Kalhor, A., & Masouleh, M.T. (2017). Dimensional synthesis of a four-bar linkage mechanism via a PSO-based Cooperative Neural Network approach. In *2017 Iranian Conference on Electrical Engineering (ICEE)* (pp. 906–911), Tehran, Iran. https://doi.org/10.1109/IranianCEE.2017.7985168

2. Buśkiewicz J. (2019). The optimum distance function method and its application to the synthesis of a gravity balanced hoist. *Mechanism and Machine Theory*, *139*, 443–459. https://doi.org/10.1016/j.mechmachtheory.2019.05.006

3. Gronowicz, A., Sperzyński, P., Szrek, J., & Jakubiak, J. (2014). Wheel-legged robot – construction and obstacle detection sensors. In V. Petuya, C. Pinto, & E.C. Lovasz (Eds.), *Mechanisms and Machine Science: Vol. 17. New Advances in Mechanisms, Transmissions and Applications* (pp. 191–198). Springer. https://doi.org/10.1007/978-94-007-7485-8_24

4. Hernández, A., Muñoyerro, A., Urízar, M., & Amezua, E. (2021). Comprehensive approach for the dimensional synthesis of a four-bar linkage based on path assessment and reformulating the error function. *Mechanism and Machine Theory*, *156*, Article 104126. https://doi.org/10.1016/j.mechmachtheory.2020.104126

5. Kang, Y.-H., Lin, J.-W., & You, W.-C. (2022). Comparative study on the synthesis of path-generating four-bar linkages using metaheuristic optimization algorithms. *Applied Sciences*, *12*(15), Article 7368. https://doi.org/10.3390/app12157368

6. Malarczyk, M., Kaczmarczyk, G., Szrek, J., & Kaminski, M. (2023). Internet of Robotic Things (IoRT) and metaheuristic optimization techniques applied for wheel-legged robot. *Future Internet*, *15*(9), Article 303. https://doi.org/10.3390/fi15090303

7. Shinde, A.S., Kulkarni, S.A., & Shete, S.S. (2017). Dimensional synthesis of mechanism using genetic algorithm. *International Journal of Current Engineering and Technology*, *7*(4), 1572–1580.

8. Wu, H., Li, X., & Yang, X. (2020). Dimensional synthesis for multi-linkage robots based on a niched Pareto genetic algorithm. *Algorithms*, *13*(9), Article 203. https://doi.org/10.3390/a13090203

Manuscript received April 10, 2024; accepted for publication February 17, 2025; published online April 22, 2025.